XI International Conference on Computational Plasticity. Fundamentals and Applications
COMPLAS 2011
E. Oñate and D.R.J. Owen (Eds)

MULTISCALE STRAIN LOCALIZATION MODELING IN THE GURSON-TVERGAARD-NEEDLEMAN PLASTICITY MODEL

SEBASTIÁN D'HERS* **AND EDUARDO DVORKIN†**

*Computational Mechanics Lab., Instituto Tecnológico de BuenosAires
Av. E. Madero 399, C1106ACD, Buenos Aires, Argentina
e-mail: sdhers@itba.edu.ar, web page: www.itba.edu.ar

† Facultad de Ingeniería , Universidad de Buenos Aires
Av. Las Heras 2214, C1127AAR Buenos Aires, Argentina web page: www.fi.uba.ar
SIM&TEC, Pueyrredón 2130, C1119ACR Buenos Aires, Argentina
e-mail: edvorkin@simytec.com, web page: www.simytec.com

Key words: Plasticity, Localization, Strong discontinuity, Multiple scales, Gurson-Tvergaard-Needleman

Abstract. The modeling of strain localization requires the use of different scales to describe the evolution of the material of the overall structure and the material inside the localized region. Focusing on the Gurson-Tvergaard-Needleman material we develop a multiscale formulation that uses strong discontinuity modes to model the development of a localization zone and the material degradation and void growth inside it. We present a strong discontinuity mode formulation able to capture the band kinematics that consists of a combination of sliding and opening modes. Then we derive an heuristic inter-scale factor to set a proper connection between the localized and the continuum scales.

This approach describes the evolution of the accumulated plastic strain and the void content inside and outside the localization band. The localization scale evolution is effectively controlled by the proposed heuristic rule. To illustrate on the formulation capabilities, a test case is presented and the behavior of the inter-scale connection factor is analyzed. The resulting formulation does not require a specific mesh refinement to model strain localization, provides mesh independent results and can be calibrated using experimental results.

1 INTRODUCTION

The Gurson-Tvergaard-Needleman plasticity model[1–5] incorporates to the standard J_2 plasticity model the material degradation that is due to the nucleation, growth and coalescence of voids. This material model is usually used for modeling ductile fracture phenomena, where the void content is used as an indicator of crack initiation.

Most ductile fracture processes are preceded by a strain localization, that takes place in a narrow band shaped region. In most cases the band width results much smaller than the problem domain, therefore forcing the two opposing sides of the region to open and/or slide relatively to each other (depending on the material considered). This inserts in the problem domain a kinematic mechanism that conditions its response.

Due to that, the modeling of strain localization phenomena via finite element formulations requires to use different scales for the description of the global deformation in the continuum and the localized deformation inside the localization bands and to use of physically meaningful laws to describe the evolution of the material inside the latter ones.

These issues have been addressed in the literature by many numerical techniques: the enhanced strain field method[6,7] the extended finite element method (X-FEM),[8,9] the strong discontinuity approach[10] and the embedded strong discontinuity modes.[11,12] The last two techniques were applied in the framework of G-T-N materials[13,14]

2 THE G-T-N MATERIAL MODEL

The Gurson plasticity model was first developed by Gurson.[1,2] It has been modified through time to adjust the model parameters[3,4] and received new inclusions like the addition of a void coalescence mechanism.[5] The complete set is known as the Gurson-Tvergaard-Needleman (G-T-N) material model. Herein we recall the equations required for the present development.[15]

The G-T-N yield surface, ${}^t\Phi$, depends on the hydrostatic stress, ${}^t\sigma_h$, the J_2 equivalent stress ${}^t\sigma_e$, the volume void fraction, ${}^t f$, and the actual yield stress,${}^t\sigma_y$, *

$$ {}^t\Phi\left({}^t\sigma_h, {}^t\sigma_e, {}^t f, {}^t\bar{\varepsilon}^P\right) = \left(\frac{{}^t\sigma_e}{{}^t\sigma_y}\right)^2 + 2\ {}^t f\ q_1\ \cosh\left(\frac{3}{2} q_2 \frac{{}^t\sigma_h}{{}^t\sigma_y}\right) - 1 - \ {}^t f\ {}^2\ q_1^2 = 0 \tag{1} $$

$$ {}^t\sigma_h = \frac{1}{3}\ {}^t\underline{\underline{\sigma}} :\ {}^t\underline{\underline{\mathbf{g}}}, \tag{2} $$

$$ {}^t\sigma_e = \sqrt{\frac{3}{2}\ {}^t\underline{\underline{\mathbf{s}}}\ :\ {}^t\underline{\underline{\mathbf{s}}}}, \tag{3} $$

being ${}^t\underline{\underline{\mathbf{s}}}$ the deviatoric stress tensor and ${}^t\underline{\underline{\mathbf{g}}}$ the metric tensor. The parameters q_1 and q_2 were set to fit the experimental results. We adopt $q_1 = 1.5$ and $q_2 = 1$ for the present study.

During yielding ${}^t\Phi = 0$; hence we can obtain an equivalent stress that takes into account the void effect,

$$ {}^t\bar{\sigma}^2 = \ {}^t\sigma_y{}^2\left(1 + \ {}^t f\ {}^2\ q_1^2 - 2\ {}^t f\ q_1\ \cosh\left({}^t\alpha\right)\right) \tag{4} $$

*We indicate the tensorial product between two tensors as a b (in other references it is indicated as $a \bigotimes b$) and the number of underlines indicates the tensor order.

For the evolution of ${}^t\sigma_y$ we adopt an implicit hardening law from,[15]

$$\frac{{}^t\sigma_y}{{}^0\sigma_y} = \left(\frac{{}^t\sigma_y}{{}^0\sigma_y} + \frac{3\ G}{{}^0\sigma_y}\ {}^t\bar{\varepsilon}^P\right)^N \tag{5}$$

where ${}^0\sigma_y$ is the initial yield stress, ${}^t\bar{\varepsilon}^P$is the equivalent plastic strain (to be defined in Eqn. (11)), N is the hardening exponent and G is the elastic shear modulus.

The increment of void volume fraction is attributed to:

- Growth of existing voids driven by the bulk plastic deformation,

$$df_{growth} = \left(1 -\ {}^t f\right)\ d\underline{\underline{\varepsilon}}^P :\ {}^t\underline{\underline{\mathbf{g}}}. \tag{6}$$

- Nucleation of new voids driven by the accumulated plastic strain evolution,[16]

$$df_{nucleation} =\ {}^t A\ d\bar{\varepsilon}^P \tag{7}$$

with:

$${}^t A = \frac{f_N}{S_N\sqrt{2\pi}} exp\left[-\frac{1}{2}\left(\frac{{}^t\bar{\varepsilon}^P - \varepsilon_N}{s_N}\right)^2\right], \tag{8}$$

where, f_N is the void volume fraction of nucleation particles, S_N its standard deviation and ε_N the mean strain for void nucleation. We adopt $s_N = 0.1$, $f_N = 0.04$ and $\varepsilon_N = 0.3$.

- Coalescence of voids is modeled by modifying ${}^t f$ once a critical void fraction, $f_{Critical}$, is reached.[5]

The evolution of the internal variables, ${}^t f$ and ${}^t\bar{\varepsilon}^P$, of the G-T-N material depends on the volumetric $\left(\varepsilon_h^P\right)$ and distortive $\left(\varepsilon_e^P\right)$ equivalent plastic strains. Those equivalent strains are defined decomposing the plastic strain increment as follows,

$$\underline{\underline{\varepsilon}}^P =\ {}^{t+\Delta t}\underline{\underline{\varepsilon}}^P -\ {}^t\underline{\underline{\varepsilon}}^P = \frac{1}{3}\varepsilon_h^P\ {}^{t+\Delta t}\underline{\underline{\mathbf{g}}} + \varepsilon_e^P\ \frac{3}{2}\frac{{}^t\underline{\underline{\mathbf{s}}}}{{}^t\sigma_e}, \tag{9}$$

Hence the increment between t and $t+\Delta t$ of the void volume fraction and the equivalent plastic strain becomes,

$${}^{t+\Delta t}f -\ {}^t f = f = \left(1 -\ {}^{t+\Delta t}f\right)\ \underline{\underline{\varepsilon}}^P :\ {}^{t+\Delta t}\underline{\underline{\mathbf{g}}} +\ {}^{t+\Delta t}A\ \bar{\varepsilon}^P, \tag{10}$$

$$\bar{\varepsilon}^P\ =\ {}^{t+\Delta t}\bar{\varepsilon}^P -\ {}^t\bar{\varepsilon}^P = \frac{{}^{t+\Delta t}\sigma_h\ \varepsilon_h^P +\ {}^{t+\Delta t}\sigma_e\ \varepsilon_e^P}{\left(1 -\ {}^{t+\Delta t}f\right)\ {}^{t+\Delta t}\sigma_y}. \tag{11}$$

3 FINITE ELEMENT FORMULATION

3.1 Displacement and strain decomposition

We solve the nonlinear elastoplastic problem using an incremental procedure where we decompose the strain and displacement increments from time t to time $t + \Delta t$ as,

$$^{t+\Delta t}\underline{\underline{\varepsilon}} = {}^{t}\underline{\underline{\varepsilon}} + \underline{\underline{\varepsilon}} \quad \wedge \quad ^{t+\Delta t}\underline{u} = {}^{t}\underline{u} + \underline{u},$$

and discretize the continuum using the standard element shape functions,[17] $\underline{\mathbf{H}}$, and the nodal displacements, $\underline{\mathbf{U}}$,

$$\underline{u} = \underline{\mathbf{H}}\ {}^{t+\Delta t}\underline{\mathbf{U}} - \underline{\mathbf{H}}\ {}^{t}\underline{\mathbf{U}} = \underline{\mathbf{H}}\underline{\mathbf{U}}.$$

At the elements where the localization indicator triggers a discontinuity, we decompose the displacement field into continuous and localized contributions,[11,12]

$$\underline{u} = \underline{u}_{continuum} + \underline{u}_{localized} = \underline{\mathbf{H}}\ \underline{\mathbf{U}}_{continuum} + \underline{\mathbf{H}}\ \underline{\mathbf{U}}_{localized} \tag{12}$$

Assuming infinitesimal strains analysis, we also decompose the deformation increment into elastic and plastic components. Since we assume the localization behaves as rigid-plastic, the elastic deformation only contributes to the continuum scale, and the plastic deformation contributes to the continuum and to the localized scales. Hence,

$$\underline{\underline{\varepsilon}} = \underline{\underline{\varepsilon}}^{E} + \underline{\underline{\varepsilon}}^{P} = \underline{\underline{\varepsilon}}^{E}_{continuum} + \underline{\underline{\varepsilon}}^{P}_{continuum} + \underline{\underline{\varepsilon}}^{P}_{localized}. \tag{13}$$

The displacement $\underline{u}_{localized}$ has to be designed as to reproduce the localized deformation kinematics, thus we adopt,[11]

$$\underline{u}_{localized} = \underline{\mathbf{H}}\ \underline{\mathbf{U}}_{localized} = \underline{\mathbf{H}}\ \gamma\ \underline{\mathbf{\Theta}} \tag{14}$$

where $\underline{\mathbf{\Theta}}$ are the nodal displacements corresponding to the strong discontinuity mode to be defined later in this work and γ is the increment of a scalar parameter which is part of the problem unknowns. The evolution of this parameter is written as,

$$^{t+\Delta t}\gamma = {}^{t}\gamma + \gamma. \tag{15}$$

Replacing Eqn. (14) into Eqn. (12) results,

$$\underline{u} = \underline{\mathbf{H}}\ \underline{\mathbf{U}} = \underline{\mathbf{H}}\,(\underline{\mathbf{U}} - \gamma\ \underline{\mathbf{\Theta}}) + \underline{\mathbf{H}}\gamma\ \underline{\mathbf{\Theta}}. \tag{16}$$

Thus the resulting strain fields, using Voight notation, are,

$$\underline{\varepsilon}_{continuum} = \underline{\varepsilon}^{E}_{continuum} + \underline{\varepsilon}^{P}_{continuum} = \underline{\mathbf{B}}\,(\underline{\mathbf{U}} - \gamma\ \underline{\mathbf{\Theta}}) \tag{17}$$

$$\underline{\varepsilon}_{localized} = \underline{\varepsilon}^{P}_{localized} = \underline{\mathbf{B}}\ \underline{\mathbf{U}}_{localized} = \underline{\mathbf{B}}\ \gamma\ \underline{\mathbf{\Theta}} \tag{18}$$

were $\underline{\mathbf{B}}$ is the adopted element strain-displacement matrix.

Summarizing this derivation, we now can build a strong discontinuity mode, $\underline{\mathbf{\Theta}}$, that can generate a localized displacement field $\underline{u}_{localized}$ with a related strain field strain $\underline{\varepsilon}^{P}_{localized}$.

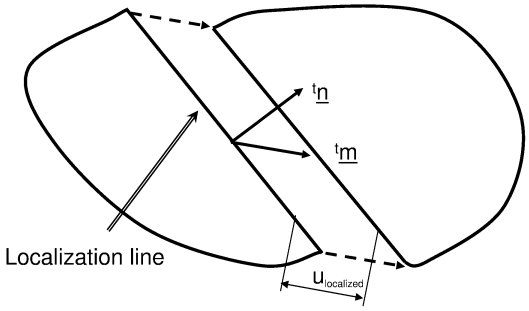

Figure 1: Continuous with an active localization.

3.2 Localization definition

A localization line in plane problems can be characterized by a line with normal ${}^t\underline{\mathbf{n}}$ and a propagation direction ${}^t\underline{\mathbf{m}}$ along which the displacement jump,[19] $\underline{u}_{localized}$, is found (i.e. if ${}^t\underline{\mathbf{n}} \parallel {}^t\underline{\mathbf{m}} \Longrightarrow$ the kinematics is Mode I and if ${}^t\underline{\mathbf{n}} \perp {}^t\underline{\mathbf{m}} \Longrightarrow$ the kinematics is Mode II). In Fig. 1 we draw a schematic representation of the above definitions, considering a general displacement jump; the band has no width.

To describe the induced localization strain we use the Maxwell conditions, so we necessitate that the discontinuity jump satisfies,[6]

$$\underline{\nabla}\ \underline{\mathbf{u}}_{localized} = \ \gamma\ {}^t\underline{\mathbf{n}}\ {}^t\underline{\mathbf{m}}$$

where γ is a scalar increment of the discontinuity jump. Hence the strain jump becomes,

$$\underline{\underline{\varepsilon}}^{P}_{localized} = \frac{1}{2}\ \gamma \left(\ {}^t\underline{\mathbf{n}}\ {}^t\underline{\mathbf{m}} + \ {}^t\underline{\mathbf{m}}\ {}^t\underline{\mathbf{n}}\right) \tag{19}$$

3.3 Bifurcation analysis

It has been shown[18,19] that the triggering of bifurcation in the material behavior and the respective band orientation can be determined from the singularity of the acoustic tensor, which is defined as,

$${}^t\underline{\underline{\mathbf{Q}}} = \ {}^t\underline{\mathbf{n}} \cdot {}^{\mathbf{t}}\underline{\underline{\underline{\underline{\mathbf{C}}}}}^{\mathbf{EP}} \cdot {}^t\underline{\mathbf{n}} \tag{20}$$

where ${}^{\mathbf{t}}\underline{\underline{\underline{\underline{\mathbf{C}}}}}^{\mathbf{EP}}$ is the constitutive tensor.

The bifurcation condition requires that,[6,18]

$${}^t\underline{\underline{\mathbf{Q}}} \cdot \ {}^t\underline{\mathbf{m}} = \ \left({}^t\underline{\mathbf{n}} \cdot {}^{\mathbf{t}}\underline{\underline{\underline{\underline{\mathbf{C}}}}}^{\mathbf{EP}} \cdot {}^t\underline{\mathbf{n}}\right) \ \cdot {}^t\underline{\mathbf{m}} = 0 \tag{21}$$

what is satisfied when,

$$\det\left({}^t\underline{\underline{\mathbf{Q}}}\right) = \det\ \left({}^t\underline{\mathbf{n}} \cdot {}^{\mathbf{t}}\underline{\underline{\underline{\underline{\mathbf{C}}}}}^{\mathbf{EP}} \cdot {}^t\underline{\mathbf{n}}\right) = 0. \tag{22}$$

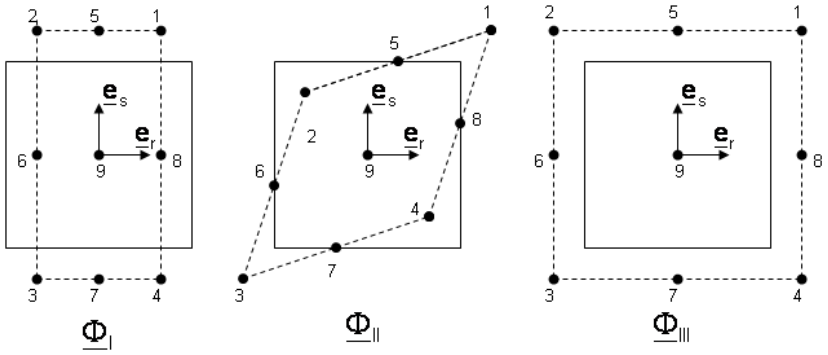

Figure 2: Base of modes for a 9-node element in the isoparametric element space.

Eqn.(22) implies that at least one of ${}^t\underline{\underline{\mathbf{Q}}}$ eigenvalues to be zero and the respective eigenvector ${}^t\underline{\mathbf{m}}$ to be the band growth direction according to Eqn.(21). Since it is difficult to precisely determine when Eqn.(22) is satisfied during an incremental procedure we use,[6]

$$\det\left({}^t\underline{\underline{\mathbf{Q}}}\right) = \det\left({}^t\underline{\mathbf{n}} \cdot {}^{\mathbf{t}}\underline{\underline{\underline{\underline{\mathbf{C}}}}}^{\mathbf{EP}} \cdot {}^t\underline{\mathbf{n}}\right) \leq 0 \tag{23}$$

and the growth direction can be obtained from the eigenvector ${}^t\underline{\mathbf{m}}$ belonging to the smallest eigenvalue of ${}^t\underline{\underline{\mathbf{Q}}}$.

3.4 Strong discontinuity modes definition

To build a strong discontinuity mode, ${}^t\underline{\mathbf{\Theta}}$, able to model the localization when scaled by γ, we use a base of displacement modes, ${}^t\underline{\mathbf{\Psi}}_A$, constituted by two shear modes and a volume change mode[11,12,14] . Subindex $A = I...III$ indicates the deformation mode.

To construct each of them, we use three different sets of nodal coordinates, ${}^t\underline{\mathbf{\Phi}}_A$, and the unstrained nodal coordinates $\left(r^k, s^k\right)$ and build them as,

$${}^t\underline{\mathbf{\Psi}}^k_A = \left[\left({}^t\Phi^k_A\right)_r - r^k\right]\ \underline{\mathbf{e}}_r\ +\ \left[\left({}^t\Phi^k_A\right)_s - s^k\right]\ \underline{\mathbf{e}}_s. \tag{24}$$

In the above equation $(\underline{\mathbf{e}}_r; \underline{\mathbf{e}}_s)$ are orthonormal base vectors shown in Fig.2 along the (r, s) natural directions and the upper index $k = 1...N$ indicates the node. As an illustrative example we plot the displacement modes in the element isoparametric space coordinates (r,s) for a 9-node element in Fig.2. To complete the definition we generalize Eqn.(24) in the (x_1, x_2) structural coordinate system using the element shape functions h_j,

$${}^t\underline{\mathbf{\Psi}}^k_A = \left[\ h_j\left(\left({}^t\Phi^k_A\right)_r, \left({}^t\Phi^k_A\right)_s\right)\ x^j_i - x^k_i\right]\underline{\mathbf{e}}_i\ . \tag{25}$$

With this displacement modes, ${}^t\underline{\mathbf{\Psi}}_A$, we compute their respective strains at the element center,

$$\underline{\varepsilon}_A = \underline{\mathbf{B}}_c\ \ {}^t\underline{\mathbf{\Psi}}_A \tag{26}$$

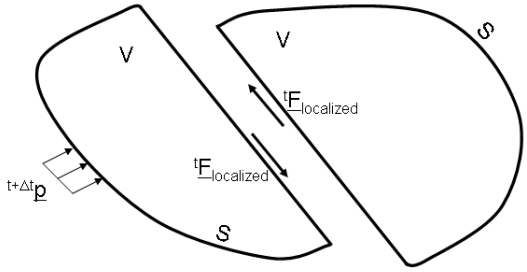

Figure 3: Continuous with an active localization band

where $\underline{\mathbf{B}}_c$ is the strain-displacements matrix calculated at the element center. By linearly combining the above defined strain fields we obtain the $\underline{\varepsilon}^P_{localized}$ defined in Eqn. (19),

$$\underline{\varepsilon}^P_{localized} = \beta_I \underline{\varepsilon}_I + \beta_{II} \underline{\varepsilon}_{II} + \beta_{III} \underline{\varepsilon}_{III} \cdot, \tag{27}$$

where β_A parameters have to be determined.

Therefore the modes ${}^t\underline{\mathbf{\Psi}}_A$ can also be linearly combined and normalized to get the localization strong discontinuity mode, ${}^t\underline{\mathbf{\Theta}}$,

$${}^t\underline{\mathbf{\Theta}} = \frac{\beta_I \ {}^t\underline{\mathbf{\Psi}}_I + \beta_{II} \ {}^t\underline{\mathbf{\Psi}}_{II} + \beta_{III} \ {}^t\underline{\mathbf{\Psi}}_{III}}{|\beta_I \ {}^t\underline{\mathbf{\Psi}}_I + \beta_{II} \ {}^t\underline{\mathbf{\Psi}}_{II} + \beta_{III} \ {}^t\underline{\mathbf{\Psi}}_{III}|} \tag{28}$$

3.5 Element equilibrium equations

We apply the virtual work principle in order to obtain the finite element equations. In Fig. 3 we show a scheme of a solid with a localization line and the localization line forces (band forces). For the equilibrium at time $t + \Delta t$ we get,

$$\int_V \delta \left[\underline{\varepsilon}_{continuum}\right]^T \ {}^{t+\Delta t}\underline{\sigma}_{continuum} \, dv \ + \ \delta \left[\underline{\mathbf{U}}_{localized}\right]^T \ {}^{t+\Delta t}\underline{\mathbf{F}}_{localized} = \int_S \delta \underline{\mathbf{u}}^T \ {}^{t+\Delta t}\underline{\mathbf{p}} \, ds. \tag{29}$$

Replacing Eqns. (12), (14) and (17) into Eqn. (29) and since $\delta\underline{\mathbf{U}}$ and $\delta\underline{\gamma}$ are arbitrary we obtain set of equations[12] that has to be solved iteratively; therefore, a Newton-Raphson scheme is implemented at the global level. The parameters γ are condensed at the element level.

The only undefined variable is ${}^{t+\Delta t}\underline{\mathbf{F}}_{localized}$ for which we propose[11] that,

$$\frac{{}^t\underline{\mathbf{\Theta}}^T \ {}^{t+\Delta t}\underline{\mathbf{F}}_{localized}}{{}^t\underline{\mathbf{\Theta}}^T \ {}^t\underline{\mathbf{F}}_{localized}} = \frac{{}^{t+\Delta t}\bar{\sigma}_{localized}}{{}^t\bar{\sigma}_{localized}}, \tag{30}$$

where the localization equivalent stress ${}^{t+\Delta t}\bar{\sigma}_{localized}$ is unknown. To calculate it, we relate the localization volumetric and distortive equivalent plastic strains to the band incremental parameter γ, through a set of positive factors ζ and φ. These factors relate the continuum and the localization scales. Hence,

$$\left(\varepsilon^P_{h \ loc}\right)^2 = \zeta^2 \gamma^2 \ , \tag{31}$$

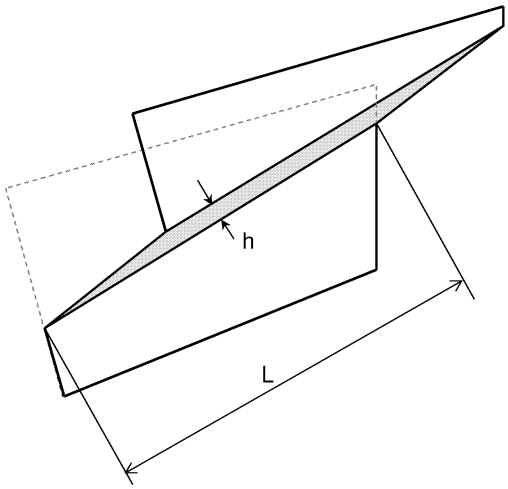

Figure 4: Scheme of a band in a localized element

$$\left(\varepsilon^P_{e\ loc}\right)^2 = \varphi^2\gamma^2. \tag{32}$$

To determine the inter-scales factors we request the distortive dissipated energy in the band to be equal to the energy dissipated by the distortive part of the localization mode. For this we calculate a purely distortive strong discontinuity mode, ${}^t\underline{\boldsymbol{\Theta}}_d$, as was done for the localization mode ${}^t\underline{\boldsymbol{\Theta}}$, hence,

$$\int_{t_\gamma}^{t+\Delta t_\gamma} \underline{\Theta}_e^T\ {}^\tau\underline{\mathbf{F}}\ d\gamma = \int_{V_{loc}} \int_{t_{\varepsilon^P_{e\ loc}}}^{t+\Delta t_{\varepsilon^P_{e\ loc}}} {}^\tau\bar{\sigma}_{loc}\ d\varepsilon^P_{e\ loc} dV_{loc}\ . \tag{33}$$

The same reasoning is applied to the hydrostatic contribution, but with the volumetric strong discontinuity mode, $\underline{\Theta}_h$.

To solve Eqn.(33) and the respective volumetric equations, we construct an heuristic rule for what we depict in Fig 4 an element shaped domain that has a localization line across it. The localization line splits the domain in two subdomains that slide along the localization line. Assuming unitary thickness, the volume of material comprised in the localization is,

$$V_{loc} = \ h\ L, \tag{34}$$

where h is a reference bandwidth and L is the band length across the element.

Using in Eqn.(33) an Euler backward time integration scheme together with Eqn. (34) and the corresponding volumetric equations leads to,

$$\gamma\ \ {}^t\underline{\Theta}_e^T\ \ {}^{t+\Delta t}\underline{\mathbf{F}}\ =\ {}^{t+\Delta t}\bar{\sigma}_{loc}\ \varepsilon^P_{e\ loc}\ h\ L\ , \tag{35}$$

and

$$\gamma\ \ {}^t\underline{\Theta}_h^T\ \ {}^{t+\Delta t}\underline{\mathbf{F}} = \ {}^{t+\Delta t}\bar{\sigma}_{loc}\ \varepsilon^P_{h\ loc}\ h\ L\ . \tag{36}$$

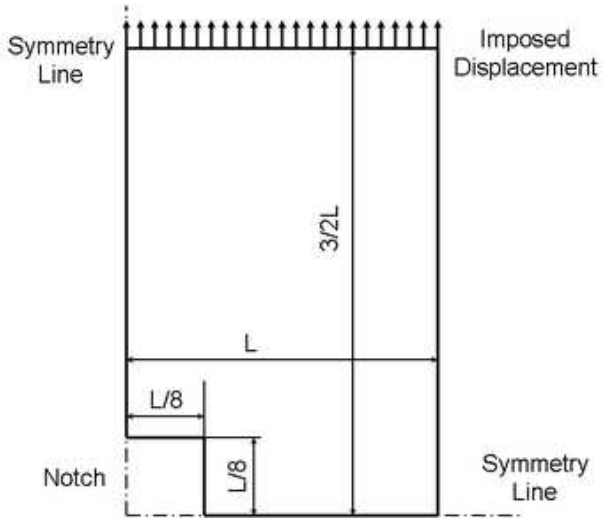

Figure 5: Test case notched sample

Replacing $\varepsilon^P_{e\ loc}$ and $\varepsilon^P_{h\ loc}$definitions into Eqns. (31) and (32) we get the inter-scales factors,

$$\varphi = \left| \frac{{}^t\underline{\boldsymbol{\Theta}}_e^T \ {}^{t+\Delta t}\underline{\mathbf{F}}_{loc}}{h\ L\ {}^{t+\Delta t}\bar{\sigma}_{loc}} \right| , \tag{37}$$

$$\zeta = \left| \frac{{}^t\underline{\boldsymbol{\Theta}}_h^T \ {}^{t+\Delta t}\underline{\mathbf{F}}}{h\ L\ {}^{t+\Delta t}\bar{\sigma}_{loc}} \right| . \tag{38}$$

Now that a proper scale is defined for the band strains, we determine $\varepsilon^P_{h_{loc}}$ and $\varepsilon^P_{e_{loc}}$ from Eqns. (31) and (32). Finally we determine the internal variables increments using Eqns. (5), (10) and (11), and replace them into Eqn. (4) to get ${}^{t+\Delta t}\bar{\sigma}_{localized}$.

The h parameter is added in Eqn. (34) to incorporate a regularization that takes into account the strain concentration inside the band. It is a bandwidth yet not a physical one. It can be interpreted as the width a band should have in order to have uniform strains inside the band with the same overall effect to the continua. This allows for parameter h to control the unloading path of the structure, as it is shown in the next section.

4 NUMERICAL EXAMPLE

To test our finite element formulation we use a plane strain pure traction test. A specimen with a central notch, used to fix the initiation of the localization, is considered as shown in Fig. 5. The element adopted for the analysis is a 4 node quadrilateral with mixed interpolated tensorial components (QMITC4)[20,21] and due to the specimen symmetry only one quarter is modeled. For time evolution we use imposed displacements with automatic time stepping up to a 4% of elongation. To focus on strain localization and not in material fracture or crack opening phenomenon, the analyzes are stopped when ${}^tf$ grows beyond 2/3. The material parameters are set to $E = 200GPa$, $\sigma_y = 600MPa$. Nor initial void volume fraction nor hardening are considered.

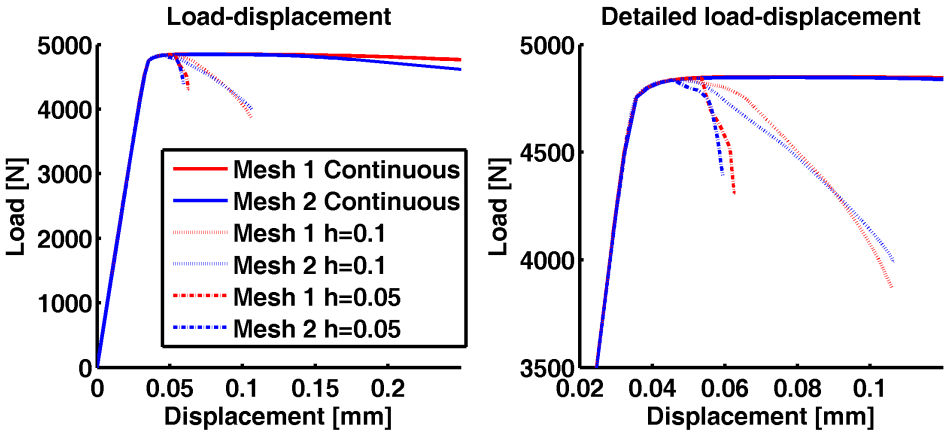

Figure 6: Load displacement results

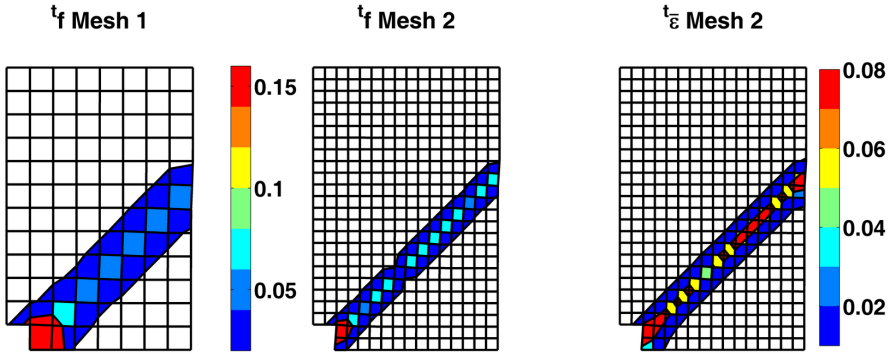

Figure 7: ${}^t f_{loc}$ and ${}^t \bar{\epsilon}^P_{loc}$ for some meshes

Two mesh densities are analyzed each for two h parameters (Eqn. 34) are used. In the load-displacement plot shown in Fig. 6 it can be seen that the use of a continuous formulation (standard finite elements) leads to mesh dependent results, while the use of the present formulation shows no mesh dependency. The parameter h has the role of scaling the material deterioration inside the band, thus controlling the load downslope. Sample band plots of the ${}^t f_{loc}$ and ${}^t \bar{\epsilon}^P_{loc}$ variables are shown in Fig. 7.

5 CONCLUSIONS

We have applied the strong discontinuity modes formulation[11,12,14] for modeling strain localization in G-T-N materials. The required inter-scales connection, between the continuum and the localization scales is achieved using an equivalent dissipated work criteria distinguishing between distortive and volumetric contributions. We introduced a length-scale (h) to heuristically model the material damage evolution inside the band. This h-parameter controls the damage-induced unloading behavior and therefore it can be determined from actual experimental data. The resulting formulation does not require a

specific mesh refinement to model a localization, provides mesh independent results and allows the control of the downslope part of the load-displacement path via the h-parameter. The actual implementation uses the same order of the Gauss integration required for calculating the element stiffness matrix and does not introduce extra d.o.f. in the assembled numerical model.

We gratefully acknowledge the support of TENARIS and ITBA for this research.

REFERENCES

[1] Gurson, A.L., *Plastic flow and fracture behavior of ductile materials incorporating void nucleation, growth and coalescence*. Ph.D. thesis, Brown University, (1975).

[2] Gurson, A.L., Continuum theory of ductile rupture by void nucleation and growth: Part 1 - yield criteria and flow rules for porous ductile materials, *J. Eng. Matl. Tech.* (1977) **99**:2-15.

[3] Tvergaard V., Influence of voids on shear band instabilities under plane strain conditions, *Int. J. Fract.* (1981) **17**:389-407.

[4] Tvergaard, V., On localization in ductile materials containing spherical voids, *Int. J. Fract.* (1982) **18**:237-252.

[5] Tvergaard, V. and Needleman, A., Analysis of the cup-cone fracture in a round tensile bar, *Acta Metallica* (1984) **32**:157-169.

[6] Ortiz, M., Leroy, Y. and Needleman, A., A Finite-Element Method for Localized Failure Analysis, *Comput. Meth. Appl. Mechs. Engng.*, (1987) **61**:189-214.

[7] Armero, F. and Garikipati K., Recent Advances in the Analysis and Numerical Simulation of Strain Localization in Inelastic Solids, *Proc. Computational Plasticity COMPLAS IV*, (Ed. by D.R.J Owen, E. Oñate and E. Hinton), Barcelona, (1995).

[8] Samaniego, E. and Belytschko, T., Continuum–discontinuum modelling of shear bands, *Int. J. Num. Methods in Engng.*, (2005), **62**:1857-1872.

[9] Areias, P.M.A. and Belytschko T., Two-scale shear band evolution by local partition of unity, *Int. J. Numerical Methods in Engng.*, (2006) **66**:878-910.

[10] Oliver, J., Modeling strong discontinuities in solid mechanics via strain softening constitutive equations. Part 1: Fundamentals, *Int. J. Numerical Methods in Engng.*, (1996) **39**:3575-3600.

[11] D'hers, S. and Dvorkin, E.N., Modeling shear bands in J2 plasticity using a two-scale formulation via embedded strong discontinuity modes, *Int. J. Numer. Meth. Engng*, (2009) **77**:1015-1043.

[12] D'hers, S. and Dvorkin, E.N.,On the modeling of shear bands formation in J2 materials with damage evolution, *Engineering Computations*, (2011) **28-2**:130-153.

[13] Sánchez, P.J. ,Huespe, A.E. and Oliver, J., On some topics for the numerical simulation of ductile fracture, *International Journal of Plasticity*, (2008), **24**:1008-1038.

[14] D'hers S., *On localization modeling for ductile materials*, Doctoral thesis, University of Buenos Aires, (2010).

[15] Aravas N., On the numerical integration of a class of pressure-dependent plasticity models, *International Journal for Numerical Methods in Engineering*, (1987) **24**:1395-1416.

[16] Chu, C.C. and Needleman, A., Void nucleation effects in bi-axially stretched sheets, *J. Eng. Mater. Technol.*, (1980) **102**:249-256.

[17] Bathe K. J., *Finite Element Procedures*, Prentice Hall, New Jersey, (1996).

[18] Rice, J.R., The Localization of Plastic Deformation, in Theoretical and Applied Mechanics, *Proceedings of the 14th International Congress on Theoretical and Applied Mechanics*, (ed. W.T. Koiter) (1976), Delft, North-Holland Publishing Co., Vol. 1, pp.207-220.

[19] Ottosen, N.S. and Runesson K., Properties of discontinuous bifurcation solutions in elasto-plasticity, *Int. J. Solids Structures*, (1991) **27**:401-421.

[20] Dvorkin, E.N. and Vassolo S.I., A quadrilateral 2D finite element based on mixed interpolation of tensorial components, *Engng. Computations*, (1989) **6**:217-224.

[21] Dvorkin, E.N., Assanelli, A.P. and Toscano R.G.,Performance of the QMITC element in 2D elasto-plastic analyzes, *Computers & Structures*, (1996) **58**:1099-1129.